

Microwave-Assisted Fabrication of Pd, Co and Ni Nanoparticles Modified-SiO₂; as Catalysts in the Reduction Reaction of Organic Pollutants

Sevtap Çağlar Yavuz^{1*} , Emre Yavuz² , Serkan Dayan³ 

^{1*} Department of Medical Services and Technicians, Ilic Dursun Yildirim Vocational School, Erzincan Binali Yildirim University, Erzincan, Türkiye

² Department of Medical Services and Technicians, Cayirli Vocational School, Erzincan Binali Yildirim University, Erzincan, Türkiye

³ Drug Application and Research Center, Erciyes University, Kayseri, Türkiye

* sevtap.yavuz@erzincan.edu.tr

* Orcid: 0000-0001-6497-2907

Received: 17 July 2023

Accepted: 26 November 2023

DOI: 10.18466/cbayarfbe.1327271

Abstract

Nanomaterials have been used in catalytic degradation of organic pollutants also act as catalysts in for many years. Due to excellent catalytic performances of metal-based nanoparticles, these materials have been used extensively in various hybrid catalyst synthesis. The main subject of this study, heterogeneous catalysis is a low cost and multi-purpose process for many pollutants. Catalytic degradation of organic pollutants such as; 2-nitrophenol, quinolin yellow and rhodamine B was investigated by using Ni, Co, Pd nanoparticles modified SiO₂ based nanomaterials. The co-doping effect on the prepared nanomaterials has been investigated with different characterization methods in terms of structural and morphological features: scanning electron microscopy, UV/vis absorption spectroscopy, energy-dispersive X-ray spectroscopy and Fourier-transform infrared spectroscopy. The highest catalytic reduction efficiencies (97.6% and 97.5%) for 2-nitrophenol and rhodamine B was obtained by Pd-PEG-AP@SiO₂ respectively. The synthesized Co-PEG-AP@SiO₂ illustrated higher catalytic reduction efficiency for quinolin yellow (70.1%) at the end of 60s. The prepared M-PEG-AP@SiO₂ nanomaterial (M: Pd,Co,Ni) can be able to utilized degradation of organic contaminants effectively.

Keywords: Catalysts, Catalytic degradation, Nanoparticles, SiO₂ nanomaterials

1. Introduction

Degradation of organic contaminants such as dyes and nitro-aromatic compounds by chemical methods can be performed quickly, simply and with high efficiency. However, removing them with new generation nanomaterials is more environmentally friendly and feasible. It is essential to combine these methods with today's nanomaterials in order to both increase the efficiency and reduce the removal costs, especially in the methods in which reducing agents such as NaBH₄, which is one of the chemical degradation methods, are used [1,2]. Catalytic degradation is an environmentally friendly technique that has emerged as a promising alternative for the remediation of various organic pollutants [3]. Heterogeneous catalyst applications are the basis of many chemical technologies used today.

The application fields of heterogeneous catalysis include chemical production, environmental technologies, energy storage and conversion [4]. Over the last decades, nanotechnology and nanomaterials have been of great interest, as it is foreseen that it will be an important step for a sustainable future. [5]. These nanoscale composites take part in numerous applications in most heterogeneous catalysis. [6-9]. Due to their high activity noble metals such as Pd, Pt, Rh [10] are often used as co-catalysts in catalytic reactions. However, because noble metals are expensive and scarce, low-cost and high-yield alternatives such as non-noble metals such as Ni and Co are highly preferred [11-16]. In recent years, the release of many toxic and harmful pollutants into the environment has increased gradually due to the rapid progress of modern industry and agriculture.

Organic pollutants in air and water, which are widely noticed among these pollutants, are potentially toxic and carcinogenic [17]. Organic dyes used in textile and food industries are an important source of environmental pollution. Dyes often have carcinogenic effects on humans and are also toxic to aquatic life [18].

Rhodamine B (Rh B) is an important xanthene dye that has many applications in textile, paper, dye and leather production [19,20]. Quinolin yellow (QY), an organic pollutant, is also a food coloring. Adsorption, oxidation, reduction, electrochemical and membrane filtration methods are widely applied to remove these pollutants in domestic and industrial wastewaters [21,22]. 2-Nitrophenol (2-NP), 3-nitrophenol (3-NP), 4-nitrophenol (4-NP) are among the most persistent organic pollutants found in wastewaters by virtue of their high stability and solubility [23]. The degradation of these contaminants have been studied for last years. In order to enhance the photocatalytic degradation performance of metal based nanoparticles (Co, Ag₂O, Pd, Cu, Ni) they should be well-decorated on templates graphene, SiO₂ etc. [24-27].

The objective of this investigation is synthesis and characterization of Pd/SiO₂, Co/SiO₂ and Ni/SiO₂ nanomaterials and using for catalytic degradation of aqueous solutions of 2-NP, QY and Rh B dyes.

2. Material and Methods

All reagents and solvents were purchased from commercial suppliers and used without further purification. The molecular interactions among the SiO₂ and metallic nanoparticles were affirmed by FT-IR (Fourier-transform infrared spectroscopy) analysis using Perkin Elmer 400 FT-IR/FT-FIR Spectrometer Spotlight 400 Imaging System. The surface morphological characterization was performed by FE-SEM (Field emission scanning electron microscopy), EDX (Energy-dispersive X-ray spectroscopy), and mapping analysis using Zeiss GeminiSEM 500. The immobilization of nanoparticles on SiO₂ was examined by X-ray diffraction (Malvern analytical XRD). The concentration of nitrophenol and dyes were determined by The UV-vis spectrophotometer (Shimadzu UV-2700).

2.1. Synthesis of Compounds

2.1.1. General Procedure for the Synthesis of Pd/SiO₂, Co/SiO₂ and, Ni/SiO₂ Nanomaterials

In order to synthesis Pd/SiO₂ nanomaterial, the previous method in literature was modified [28]. 0.5 g 3-amino functionalized silica gel, 0.025 g PEG P123 and 0.0886 g PdCl₂ were weighted and dissolved in 20 ml ultrapure water. After that this mixture was transferred into 25 ml Teflon-lined stainless steel

hydrothermal unit. The hydrothermal unit was heated in microwave oven at 600 W for 10 minute and then cooled to room temperature. 0.0378 g NaBH₄ was added to this mixture and was heated in microwave oven at 600 W for 10 minutes again. The precipitates were filtered and washed with ultrapure water, ethanol, respectively. The obtained nanomaterial was dried at 60 °C at for 3 hours.

For synthesis of Co/SiO₂ and Ni/SiO₂ nanomaterials, Co(NO₃)₂.6H₂O (0.1455 g) and Ni(NO₃)₂.6H₂O (0.1454 g) was weighted and the similar procedure that described above was performed.

2.2. Model Reduction Reaction with Fabricated Catalysts

The catalytic efficiencies of Pd-PEG-AP@SiO₂, Co-PEG-AP@SiO₂, and Ni-PEG-AP@SiO₂ nanoparticles were investigated about reduction reaction process and the 2-NP, QY, and Rh B were selected as reduced organic pollutants with BH₄⁻ ion (in the optimum concentration) at ambient temperature in water. In brief, firstly, the Pd-PEG-AP@SiO₂, Co-PEG-AP@SiO₂, and Ni-PEG-AP@SiO₂ nanoparticles (5 mg) prepared and added to the reaction tube with the organic pollutants solution and NaBH₄ (0.03 M) as a hydrogen source in water (10 ml) at ambient temperature and different times. End of the desired time, the measurement example (approximately 2.5 ml) from the catalytic reaction were filtered through the micro-column with cotton for UV-vis spectrophotometer measurements in different nm range. The catalytic performances of Pd-PEG-AP@SiO₂, Co-PEG-AP@SiO₂, and Ni-PEG-AP@SiO₂ nanoparticles were monitored the absorption bands relating organic pollutants and the corresponding peaks were seen appeared and disappeared after reduction process on the UV-vis spectrum.

3. Results and Discussion

3.1. Synthesis and Characterization

FT-IR

The molecular interaction that occurred in the Pd-PEG-AP@SiO₂, Co-PEG-AP@SiO₂, and Ni-PEG-AP@SiO₂ nanoparticles were verified by infrared spectroscopy (FT-IR). The spectra of Pd-PEG-AP@SiO₂, Co-PEG-AP@SiO₂, and Ni-PEG-AP@SiO₂ nanoparticles are given in Figure 1 and the data of spectrums of nanoparticles are listed as follows;

For Pd-PEG-AP@SiO₂, FT-IR (cm⁻¹): 3292, 2980, 2941, 2878, 1709, 1620, 1565, 1549, 1515, 1403, 1338, 1048, 795, 784, 712, 704, 693, 682, 674, 660, 650, 619, 607, 602, 589, 574, 561, 547, 536, 520, 513, 451, 444, 435, 426, 418, 407, 402.

For Co-PEG-AP@SiO₂, FT-IR (cm⁻¹): 3683, 3675, 3664, 2988, 2972, 2901, 1451, 1406, 1394, 1383, 1249, 1241, 1229, 1225, 1074, 1066, 1056, 1050, 1028, 893, 880, 788, 745, 720, 709, 704, 685, 674, 666, 648, 638, 633, 626, 601, 590, 578, 570, 559, 554, 542, 530, 518, 513, 493, 471, 463, 454, 441, 433, 424, 417, 408.

For Ni-PEG-AP@SiO₂, FT-IR (cm⁻¹): 3684, 3675, 3661, 2988, 2972, 2901, 1626, 1451, 1406, 1394, 1382, 1249, 1241, 1226, 1066, 1054, 1028, 893, 880, 799, 789, 753, 744, 675, 668, 626, 602, 578, 570, 554, 539, 532, 526, 520, 471, 464, 449, 441, 430, 419, 412. According to the FT-IR data, the N-H/O-H, C-H (aliphatic) stretching bands were obtained between ≈ 3650-3200 cm⁻¹, ≈ 3100-2800 cm⁻¹, respectively. Also, the Si-O-Si and Si-O bands were assigned as 1150-1000 cm⁻¹ and 600-450 cm⁻¹, respectively. Thus, the molecular structure of the fabricated nanomaterials is compatible with the FT-IR data (Figure 1).

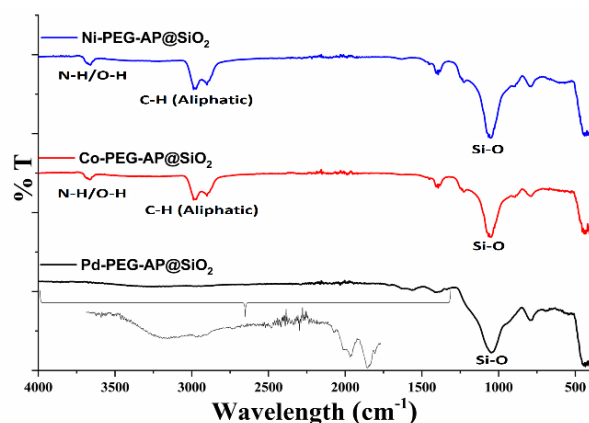


Figure 1. FT-IR spectra of the fabricated Pd-PEG-AP@SiO₂, Co-PEG-AP@SiO₂, and Ni-PEG-AP@SiO₂ nanoparticles.

XRD

The X-ray diffraction pattern of the Pd-PEG-AP@SiO₂, Co-PEG-AP@SiO₂, and Ni-PEG-AP@SiO₂ are given in Figure 2.

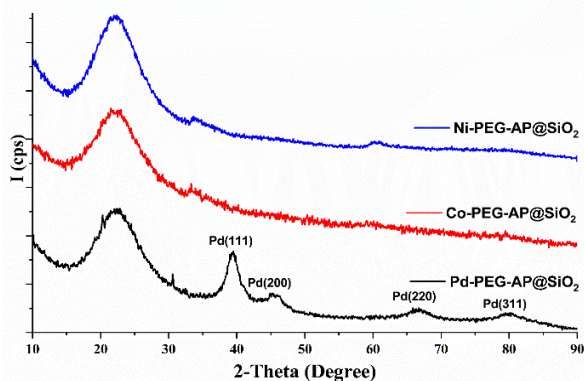


Figure 2. XRD pattern of the fabricated Pd-PEG-AP@SiO₂, Co-PEG-AP@SiO₂, and Ni-PEG-AP@SiO₂ nanoparticles.

The pattern of Pd-PEG-AP@SiO₂ was matched with JCPDS card: 87-064, but for other materials, the amorphous SiO₂ structure was recorded as the dominant pattern (Figure 2).

SEM-EDX

The field emission scanning electron microscopy (FE-SEM), EDX, and Pd, Co, and Ni mapping analyses of Pd-PEG-AP@SiO₂, Co-PEG-AP@SiO₂, and Ni-PEG-AP@SiO₂ were carried out, and the surface morphologies, EDX, and elemental images are given in Figure 3-5. When the surface morphologies were examined, it was noted that the material containing Pd had a granular structure compared to other materials. It was observed that the materials containing Co and Ni formed a sheet-like morphology as shown in Figure 3. Considering the EDX images, the Si, C, O, N, Pd, Co, and Ni elements were registered as conforming to the structure. The presence of palladium, cobalt, nickel metals (Pd weight: ≈3.7%, Co weight: ≈2.7%, and Ni weight: ≈2.5% with EDX analysis) dispersed on Pd-PEG-AP@SiO₂, Co-PEG-AP@SiO₂, and Ni-PEG-AP@SiO₂ were confirmed by the EDX and elemental mapping method (Figure 4-5).

3.2. Catalytic Studies

We examined the catalytic performances of Pd-PEG-AP@SiO₂, Co-PEG-AP@SiO₂, and Ni-PEG-AP@SiO₂ nanoparticles by using the reduction of 2-NP, QY and Rh B in the presence of sodium borohydride (NaBH₄) and deionized water at the ambient temperature. The performances of catalysts were monitored by UV-vis spectrophotometer due to the 2-nitrophenolate molecule (λ_{max}= 414 nm). In the reduction of 2-NP, the solution of 2-NP (5.00E-04M) has a yellow colour of the absorption band from the 2-nitrophenolate molecule, and the colour gradually vanished due to the reaction product (2-aminophenol).

The catalytic performances were obtained as time-dependent between 10-180 s. The catalytic efficiencies of nanoparticles were achieved as 22.4%, 48.3%, and 97.6% for Pd-PEG-AP@SiO₂, 11.1%, 22.4%, and 73.1% for Co-PEG-AP@SiO₂, 11.0%, 11.1%, and 13.5% for Ni-PEG-AP@SiO₂ at the end of 10, 60, and 180 s, respectively (Figure 6).

Similarly, we were worked the reduction of QY (6.60E-05 M) and Rh B (2.09E-05 M) dyes by Pd-PEG-AP@SiO₂, Co-PEG-AP@SiO₂, and Ni-PEG-AP@SiO₂ nanoparticles under the same conditions.

For the reduction of QY, the absorption band at 414 nm disappeared as time-dependent between 10-60 s with the catalysts. The catalytic conversions were recorded as 29.2%, 36.0%, and 62.9% for Pd-PEG-AP@SiO₂, 66.9%, 67.1%, and 70.1% for Co-PEG-

AP@SiO₂, 58.6%, 59.8%, and 64.7% for Ni-PEG-AP@SiO₂ at the end of 10, 30, and 60 s, respectively (Figure 7).

We have also worked on the reduction of Rh B, the absorption band at 550 nm disappeared during the catalytic reaction. The conversions were founded as 95.1%, 96.6%, and 97.5% for Pd-PEG-AP@SiO₂, 36.0%, 39.7%, and 40.8% for Co-PEG-AP@SiO₂, 28.1%, 28.9%, and 34.4% for Ni-PEG-AP@SiO₂ at the end of 10, 30, and 60 s, respectively (Figure 8).

In addition, the kinetic equation for the catalytic reaction of organic pollutants can be represented as $\ln(C_t/C_0) = -kt$, where t is time for the catalytic reaction and, k is the apparent first-order rate constant (s^{-1}) in Table 1. Also, the $k' = k/M$ parameter (M : the amount of the catalyst) is introduced for quantitative comparison and the parameter is defined as the ratio of the rate constant k to the weight of the catalyst added [29].

The reaction rate constant parameters were compared for the fabricated Pd-PEG-AP@SiO₂, Co-PEG-AP@SiO₂, and Ni-PEG-AP@SiO₂ nanoparticles and as time-dependend. Our palladium-containing nanomaterial (Pd-PEG-AP@SiO₂) was found to be highly effective when compared with catalysts made from similar substrates in the literature (Table-1).

According to the obtained data, the Pd-PEG-AP@SiO₂ nanoparticle was recorded as the most effective catalyst overall. However, it was noted that the Co-PEG-AP@SiO₂ nanoparticle performed better in the QY reduction reaction. The development of hybrid materials and their performance in catalytic reactions have gained importance in recent years. Also, the development of low-cost and one-pot materials is attracting more attention. Although the catalytic performance of rare elements (Pd, Ru, Pt etc.) is high, the catalytic performance of other metals is also frequently investigated. In particular, the development of materials containing other metals is supported by researchers.

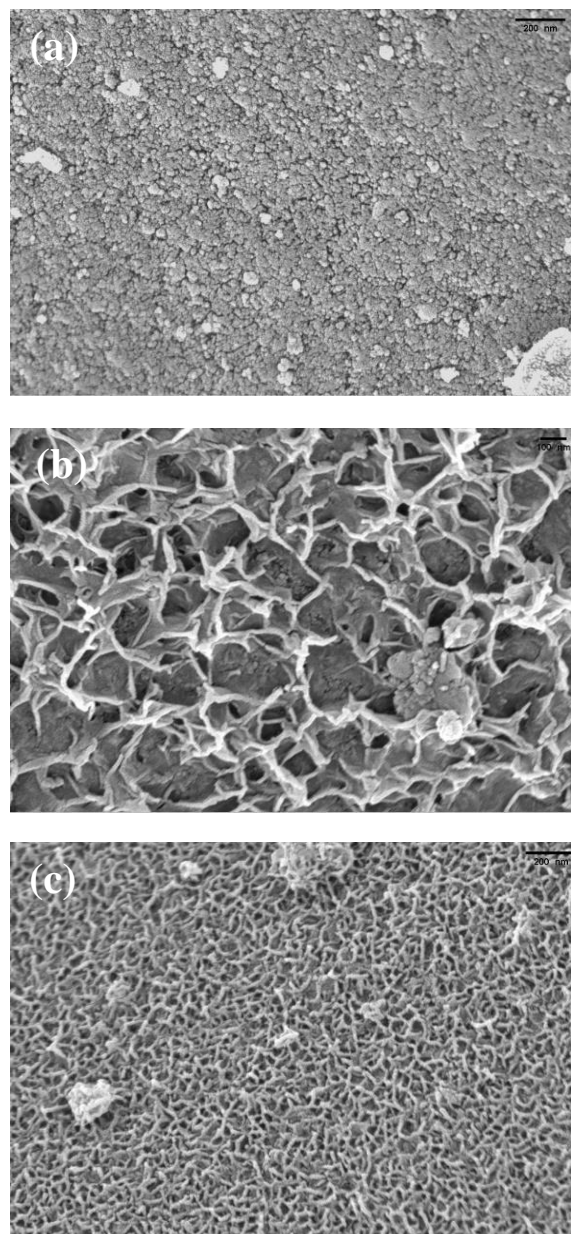


Figure 3. SEM images (50.00 KX) of the fabricated Pd-PEG-AP@SiO₂ (a), Co-PEG-AP@SiO₂ (b), and Ni-PEG-AP@SiO₂ (c) nanoparticles, respectively.

Herein, the good performance with the fabricated nanoparticles were achieved in the reduction of some organic pollutants such as 2-NP, QY and Rh B which it is known that the dyes are serious environmental pollutants. The reduction or removal of these type molecules is very important. The hybrid materials can be easily produced to reduce these harmful compounds with high activity.

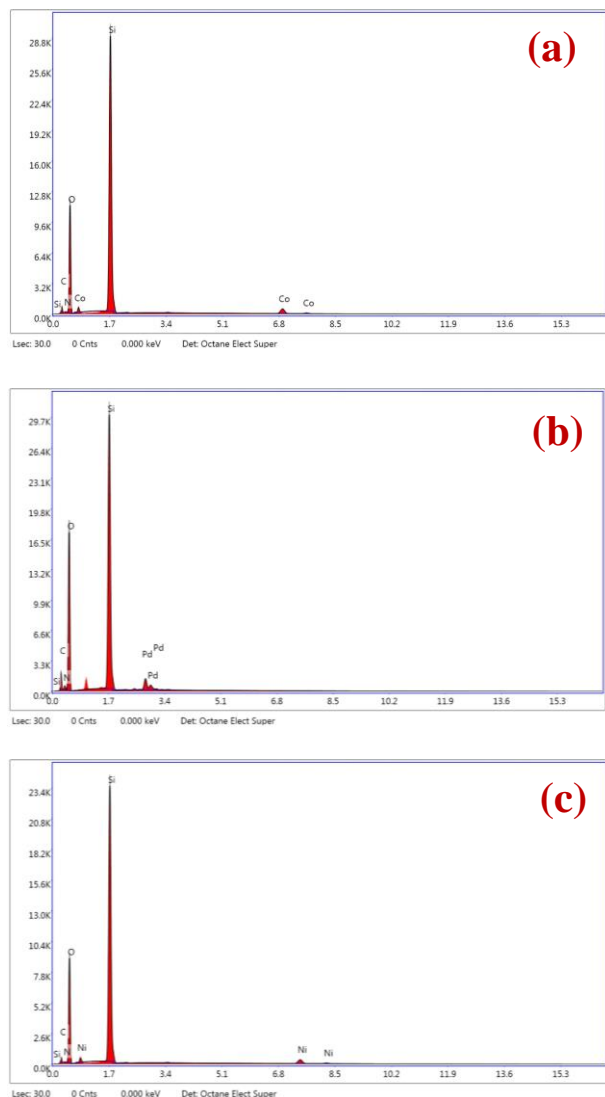


Figure 4. EDX images of the fabricated Pd-PEG-AP@SiO₂ (a), Co-PEG-AP@SiO₂ (b), and Ni-PEG-AP@SiO₂ (c) nanoparticles, respectively.

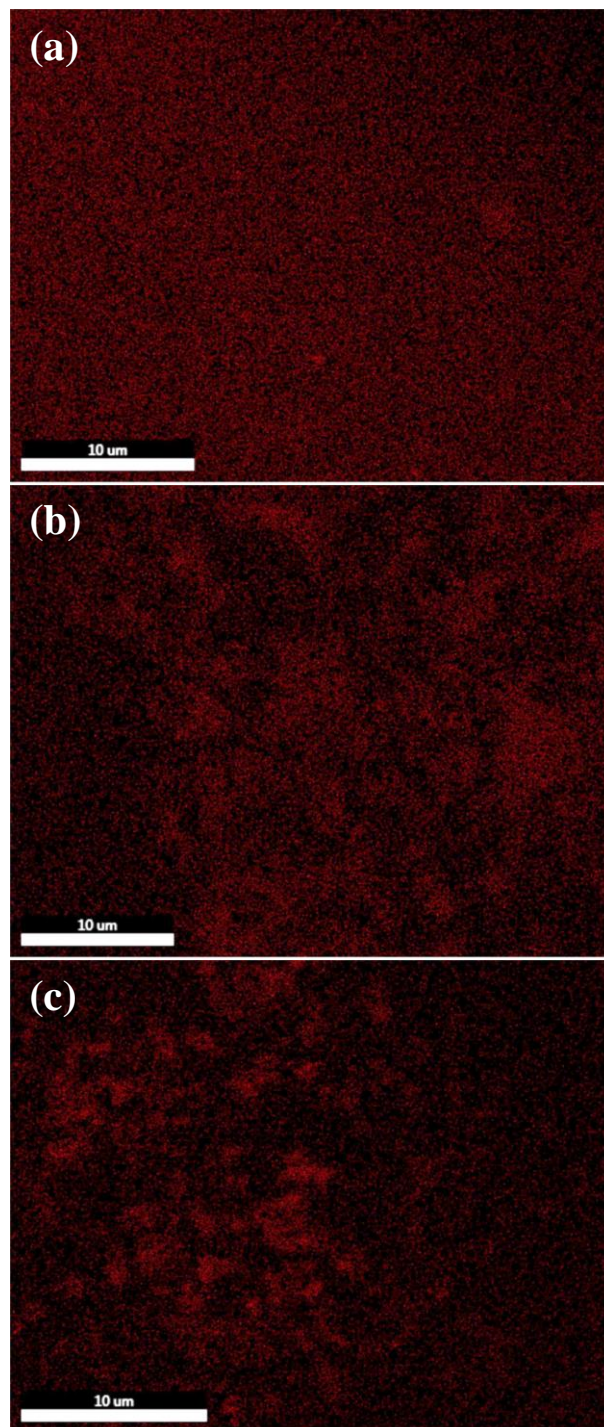


Figure 5. EDX-mapping images of the fabricated Pd-PEG-AP@SiO₂ (a) (Pd mapping), Co-PEG-AP@SiO₂ (b) (Co mapping), and Ni-PEG-AP@SiO₂ (c) (Ni mapping) nanoparticles, respectively

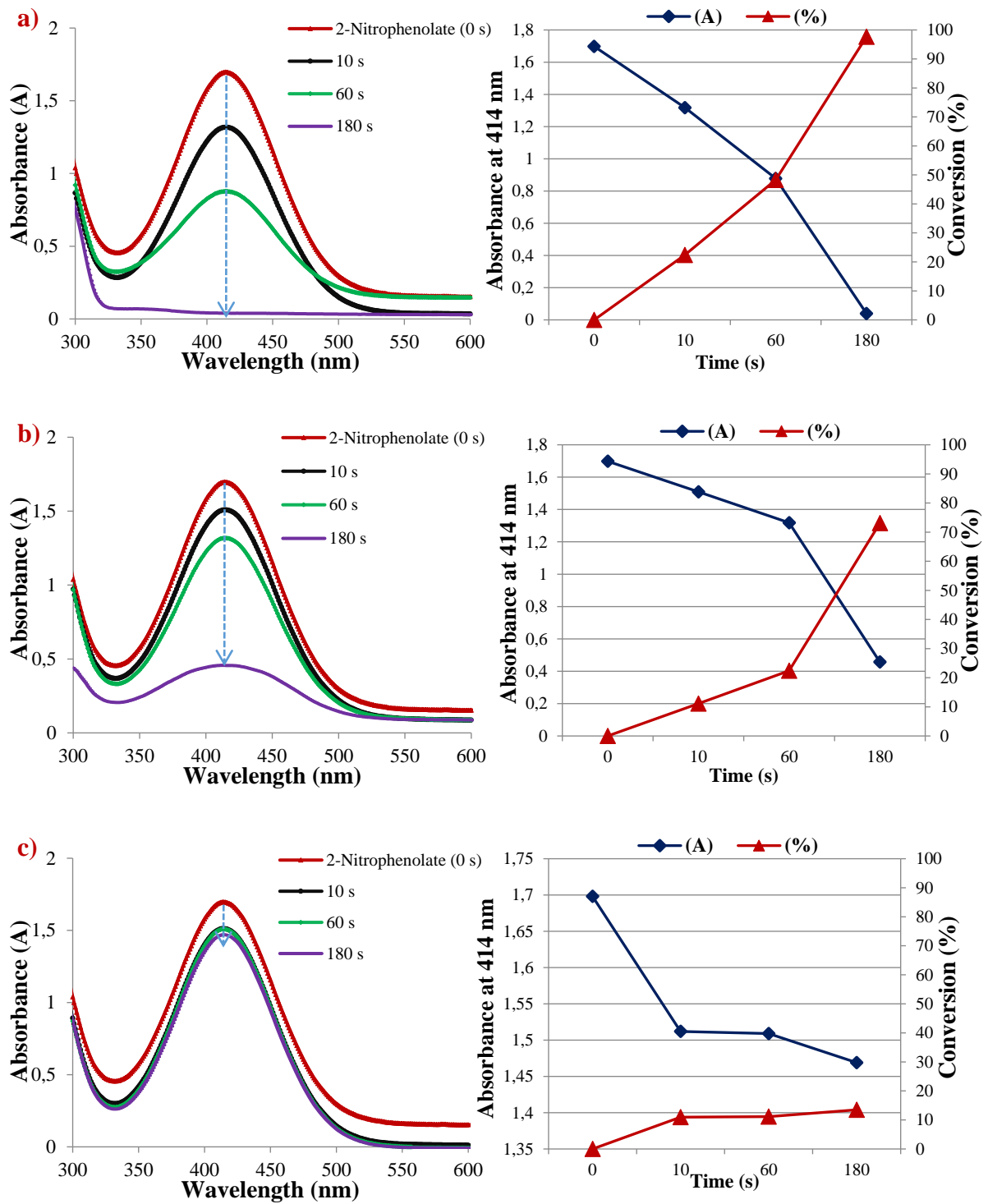


Figure 6. Time-dependent UV-vis absorption spectra of the 2-NP ($5.00E-04$ M) reduced by NaBH_4 catalyzed by Pd-PEG-AP@SiO₂ (a), Co-PEG-AP@SiO₂ (b), and Ni-PEG-AP@SiO₂ (c) nanoparticles, respectively.

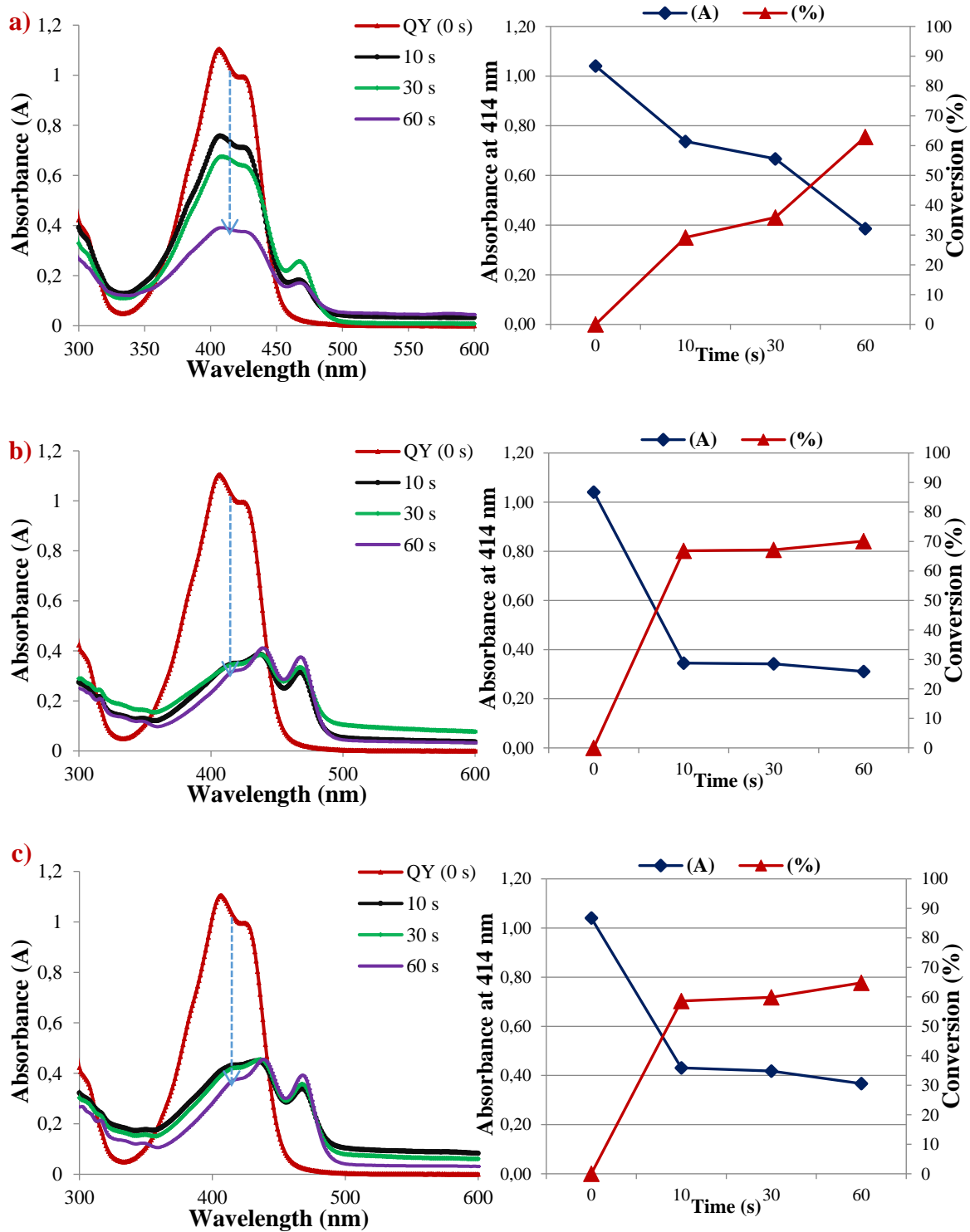


Figure 7. Time-dependent UV-vis absorption spectra of the QY ($6.60\text{E-}05\text{ M}$) reduced by NaBH_4 catalyzed by Pd-PEG-AP@SiO₂ (a), Co-PEG-AP@SiO₂ (b), and Ni-PEG-AP@SiO₂ (c) nanoparticles, respectively.

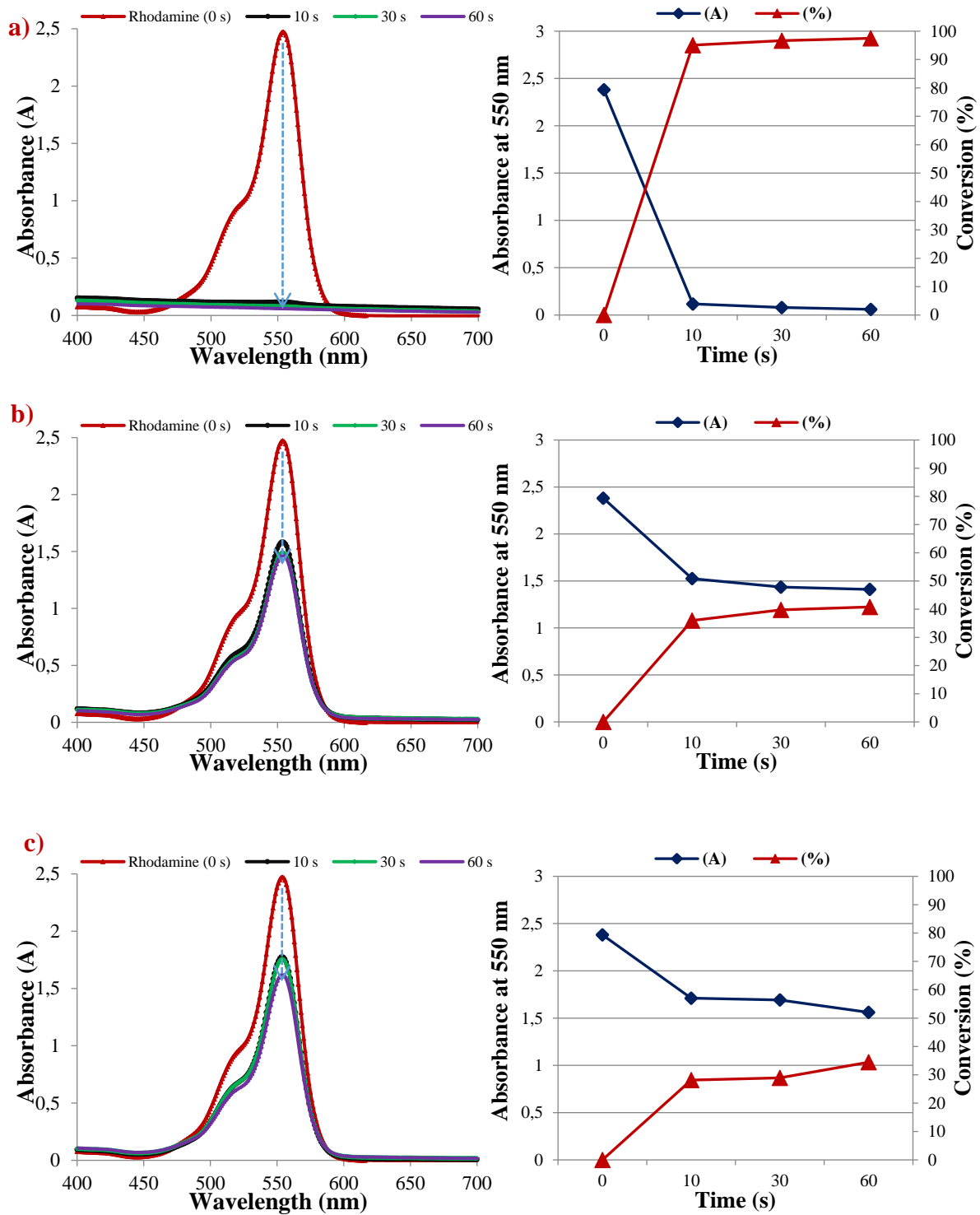


Figure 8. Time-dependent UV-vis absorption spectra of the Rh B (10 ppm (2.09×10^{-5} M)) reduced by NaBH_4 catalyzed by Pd-PEG-AP@SiO₂ (a), Co-PEG-AP@SiO₂ (b), and Ni-PEG-AP@SiO₂ (c) nanoparticles, respectively.

Table 1. The catalytic efficiency rate constant of Pd-PEG-AP@SiO₂, Co-PEG-AP@SiO₂, and Ni-PEG-AP@SiO₂ catalysts.

Catalyst	Substrate	k (s ⁻¹) ^a			k/M (s ⁻¹ g ⁻¹) ^b		
Pd-PEG-AP@SiO ₂	2-NP	2.53E-02 ^c	1.10E-02 ^e	2.08E-02 ^f	5.07E+00 ^c	2.20E+00 ^e	4.16E+00 ^f
Co-PEG-AP@SiO ₂	2-NP	1.18E-02 ^c	4.22E-03 ^e	7.29E-03 ^f	2.36E+00 ^c	8.44E-01 ^e	1.46E+00 ^f
Ni-PEG-AP@SiO ₂	2-NP	1.16E-02	1.97E-03	8.05E-04	2.32E+00	3.93E-01	1.61E-01
Pd-PEG-AP@SiO ₂	QY	3.45E-02 ^c	1.48E-02 ^d	1.65E-02 ^e	6.91E+00 ^c	2.97E+00 ^d	3.31E+00 ^e
Co-PEG-AP@SiO ₂	QY	1.10E-01 ^c	3.71E-02 ^d	2.01E-02 ^e	2.21E+01 ^c	7.42E+00 ^d	4.03E+00 ^e
Ni-PEG-AP@SiO ₂	QY	8.82E-02 ^c	3.04E-02 ^d	1.74E-02 ^e	1.76E+01 ^c	6.08E+00 ^d	3.48E+00 ^e
Pd-PEG-AP@SiO ₂	Rh B	3.01E-01 ^c	1.13E-01 ^d	6.13E-02 ^e	6.03E+01 ^c	2.26E+01 ^d	1.23E+01 ^e
Co-PEG-AP@SiO ₂	Rh B	4.46E-02 ^c	1.69E-02 ^d	8.73E-03 ^e	8.91E+00 ^c	3.38E+00 ^d	1.75E+00 ^e
Ni-PEG-AP@SiO ₂	Rh B	3.30E-02 ^c	1.14E-02 ^d	7.04E-03 ^e	6.61E+00 ^c	2.28E+00 ^d	1.41E+00 ^e
Cu/Ligand@Fullerene [30]	Rh B	9.31E-03 (120 s)	7.52E-03 (240 s)	6.58E-03 (360 s)	3.72E+00 (120 s)	3.01E+00 (240 s)	2.63E+00 (360 s)
Cu/Ligand@Fullerene [30]	2-NP	1.39E-02 (30 s)	1.46E-02 (90 s)	6.78E-03 (300 s)	5.57E+00 (30 s)	5.83E+00 (90 s)	2.71E+00 (300 s)
Co ₃ O ₄ @nHAP [31]	Rh B	2.74E-03 (90 s)	1.94E-03 (240 s)	2.24E-03 (900 s)	9.13E-01 (90 s)	6.45E-01 (240 s)	7.47E-01 (900 s)
Co ₃ O ₄ @nHAP [31]	2-NP	4.03E-03 (180 s)	7.31E-03 (360 s)	5.27E-03 (540 s)	1.34E+00 (180 s)	2.44E+00 (360 s)	1.76E+00 (540 s)

^aThe reaction rate constant. ^bThe reaction rate constant per total weight of tested catalyst (5 mg). ^c 10 s, ^d 30 s, ^e 60 s, ^f 180 s.

4. Conclusion

The M-PEG-AP@SiO₂ nanomaterial (M: Pd, Co, Ni) was prepared by a facile hydrothermal route in order to degradation of organic contaminants effectively. The obtained nanocatalysts were characterized by XRD, SEM, EDX, FT-IR techniques. The synthesized Pd-PEG@SiO₂ nanomaterial have illustrated outstanding catalytic performance for 2-NP (97.6% conversion) and Rh B (97.5% conversion) degradation. In addition, the Co-PEG-AP@SiO₂ catalysts also showed the best catalytic performance for QY after 60 seconds (70.1% conversion). Owing to the obtained results, the proposed nano catalyst can be able utilized for remediation of contaminated environmental water samples by organic contaminants such as dyes and toxic aromatic compounds.

Author's Contributions

Sevtap Çağlar Yavuz: Investigation, Data Curation, Methodology, Project administration, Writing - review & editing, Formal analysis, Funding acquisition

Emre Yavuz: Investigation, Methodology, Data Curation, Writing-original draft, Project administration

Serkan Dayan: Methodology, Data Curation, Project administration, Writing - review & editing, Formal analysis, Funding acquisition

Ethics

There are no ethical issues after the publication of this manuscript.

5. References

- [1]. Da'na, E., Taha, A., El-Aassar, M. R. 2023. Catalytic reduction of p-nitrophenol on MnO₂/zeolite-13X prepared with lawsonia inermis extract as a stabilizing and capping agent. *Nanomaterials*, 13(4): 785.
- [2]. Kumar, R., Barakat, M., Daza, Y., Woodcock, H., Kuhn, J. 2013. EDTA functionalized silica for removal of Cu (II), Zn (II) and Ni (II) from aqueous solution. *Journal of Colloid and Interface Science*, 408, 200–205.
- [3]. Fu, Y., Yin, Z., Qin, L., Huang, D., Yi, H., Liu, X., Liu, S., Zhang, M., Li, B., Li, L., Wang, W., Zhou, X., Li, Y., Zeng, G., Lai, C. 2022. Recent progress of noble metals with tailored features in catalytic oxidation for organic pollutants degradation. *Journal of Hazardous Materials*, 422, 126950.
- [4]. Ertl, G., Knözinger, H., Weitkamp, J. (Eds.). 1997. Weinheim: VCH. Handbook of heterogeneous catalysis. 2, 427-440.
- [5]. Colmenares, J. C., Luque, R., Campelo, J. M., Colmenares, F., Karpinski, Z., Romero, A. A. 2009. Nanostructured photocatalysts and their applications in the photocatalytic transformation of lignocellulosic biomass: an overview. *Materials*, 2(4): 2228-2258.
- [6]. Hurley, K. D., Shapley, J. R. 2007. Efficient heterogeneous catalytic reduction of perchlorate in water. *Environmental Science & Technology*, 41(6): 2044-2049.
- [7]. Kim, K. H., Ihm, S. K. 2011. Heterogeneous catalytic wet air oxidation of refractory organic pollutants in industrial wastewaters: a review. *Journal of Hazardous Materials*, 186(1): 16-34.
- [8]. Yao, Y., Cai, Y., Lu, F., Wei, F., Wang, X., Wang, S. 2014. Magnetic recoverable MnFe₂O₄ and MnFe₂O₄-graphene hybrid as heterogeneous catalysts of peroxydisulfate activation for efficient degradation of aqueous organic pollutants. *Journal of Hazardous Materials*, 270, 61-70.
- [9]. Wang, J., Zhang, J., Song, Y., Xu, X., Cai, M., Li, P., Yuan, W., Xiahou, Y. 2023. Functionalized agarose hydrogel with in situ Ag nanoparticles as highly recyclable heterogeneous catalyst for aromatic organic pollutants. *Environmental Science and Pollution Research*, 30(15): 43950-43961



- [10]. Kim, H. S., Kim, H. J., Kim, J. H., Kim, J. H., Kang, S. H., Ryu, J. H., Park, N. K., Yun, D. S., Bae, J. W. 2022. Noble-metal-based catalytic oxidation technology trends for volatile organic compound (VOC) removal. *Catalysts*, 12(1): 63.
- [11]. Cao, S., Wang, C. J., Lv, X. J., Chen, Y., Fu, W. F. 2015. A highly efficient photocatalytic H₂ evolution system using colloidal CdS nanorods and nickel nanoparticles in water under visible light irradiation. *Applied catalysis B: Environmental*, 162, 381-391.
- [12]. Han, G., Jin, Y. H., Burgess, R. A., Dickenson, N. E., Cao, X. M., Sun, Y. 2017. Visible-light-driven valorization of biomass intermediates integrated with H₂ production catalyzed by ultrathin Ni/CdS nanosheets. *Journal of the American Chemical Society*, 139(44): 15584-15587.
- [13]. Wang, P., Xu, S., Chen, F., Yu, H. 2019. Ni nanoparticles as electron-transfer mediators and NiS_x as interfacial active sites for coordinative enhancement of H₂-evolution performance of TiO₂. *Chinese Journal of Catalysis*, 40(3): 343-351.
- [14]. Zhang, Y., Jin, Z., Yuan, H., Wang, G., Ma, B. 2018. Well-regulated nickel nanoparticles functional modified ZIF-67 (Co) derived Co₃O₄/CdS pn heterojunction for efficient photocatalytic hydrogen evolution. *Applied Surface Science*, 462, 213-225.
- [15]. Chai, Z., Zeng, T. T., Li, Q., Lu, L. Q., Xiao, W. J., Xu, D. 2016. Efficient visible light-driven splitting of alcohols into hydrogen and corresponding carbonyl compounds over a Ni-modified CdS photocatalyst. *Journal of the American Chemical Society*, 138(32): 10128-10131.
- [16]. Simon, T., Bouchonville, N., Berr, M. J., Vaneski, A., Adrović, A., Volbers, D., Wyrwich, R., Döblinger, M., Susha, A. S., Rogach, A. L., Jackel, F., Stolarczyk, J. K., Feldmann, J. 2014. Redox shuttle mechanism enhances photocatalytic H₂ generation on Ni-decorated CdS nanorods. *Nature Materials*, 13(11): 1013-1018.
- [17]. Kim, B., Lee, Y. R., Kim, H. Y., Ahn, W. S. 2018. Adsorption of volatile organic compounds over MIL-125-NH₂. *Polyhedron*, 154, 343-349.
- [18]. Baughman, G. L., Weber, E. J. 1994. Transformation of dyes and related compounds in anoxic sediment: kinetics and products. *Environmental Science & Technology*, 28(2): 267-276.
- [19]. Isari, A. A., Payan, A., Fattahi, M., Jorfi, S., Kakavandi, B. 2018. Photocatalytic degradation of rhodamine B and real textile wastewater using Fe-doped TiO₂ anchored on reduced graphene oxide (Fe-TiO₂/rGO): Characterization and feasibility, mechanism and pathway studies. *Applied Surface Science*, 462, 549-564.
- [20]. Basturk, E., Karatas, M. 2015. Decolorization of anthraquinone dye Reactive Blue 181 solution by UV/H₂O₂ process. *Journal of Photochemistry and Photobiology A: Chemistry*, 299, 67-72.
- [21]. Qin, J., Zhang, Q., Chuang, K. T. 2001. Catalytic wet oxidation of p-chlorophenol over supported noble metal catalysts. *Applied Catalysis B: Environmental*, 29(2): 115-123.
- [22]. Fujitani, T., Nakamura, J. 2000. The chemical modification seen in the Cu/ZnO methanol synthesis catalysts. *Applied Catalysis A: General*, 191(1-2): 111-129.
- [23]. Di Paola, A., Augugliaro, V., Palmisano, L., Pantaleo, G., Savinov, E. 2003. Heterogeneous photocatalytic degradation of nitrophenols. *Journal of Photochemistry and Photobiology A: Chemistry*, 155(1-3): 207-214.
- [24]. Naeem, H., Ajmal, M., Khatoun, F., Siddiq, M., Khan, G. S. 2021. Synthesis of graphene oxide-metal nanoparticle nanocomposites for catalytic reduction of nitrocompounds in aqueous medium. *Journal of Taibah University for Science*, 15(1), 493-506.
- [25]. Kamal, T., Asiri, A. M., Ali, N. 2021. Catalytic reduction of 4-nitrophenol and methylene blue pollutants in water by copper and nickel nanoparticles decorated polymer sponges. *Spectrochimica Acta Part A: Molecular and Biomolecular Spectroscopy*, 261, 120019-120028.
- [26]. Veisi, H., Ozturk, T., Karmakar, B., Tamoradi, T., Hemmati, S. 2020. In situ decorated Pd NPs on chitosan-encapsulated Fe₃O₄/SiO₂-NH₂ as magnetic catalyst in Suzuki-Miyaura coupling and 4-nitrophenol reduction. *Carbohydrate polymers*, 235, 115966-115973.
- [27]. Nurwahid, I. H., Dimonti, L. C. C., Dwiatmoko, A. A., Ha, J. M., Yunarti, R. T. 2022. Investigation on SiO₂ derived from sugarcane bagasse ash and pumice stone as a catalyst support for silver metal in the 4-nitrophenol reduction reaction. *Inorganic Chemistry Communications*, 135, 109098-109108.
- [28]. Pal, J., Deb, M. K., Deshmukh, D. K., Sen, B. K. 2014. Microwave-assisted synthesis of platinum nanoparticles and their catalytic degradation of methyl violet in aqueous solution. *Applied Nanoscience*, 4, 61-65.
- [29]. Baghbamidi, S. E., Hassankhani, A., Sanchooli, E., Sadeghzadeh, S.M. 2018. The reduction of 4-nitrophenol and 2-nitroaniline by palladium catalyst based on a KCC-1/IL in aqueous solution. *Applied Organometallic Chemistry*, 32(4): e4251.
- [30]. Dayan, S. Copper Nanoparticles Supported on a Schiff base-Fullerene as Catalyst for Reduction of Nitrophenols and Organic Dyes. *Celal Bayar University Journal of Science*, 16 (3), 285-291.
- [31]. Dayan, S. Performance improvement of Co₃O₄@ nHAP hybrid nanomaterial in the UV light-supported degradation of organic pollutants and photovoltaics as counter electrode. *Journal of Molecular Structure*, 1238, 130390.